Iranica Journal of Energy & Environment
Journal Homepage: www.ijee.net
IJEE an official peer review journal of Babol Noshirvani University of Technology, ISSN:2079-2115

Adsorptive Removal of Methylene Blue Dye from Aqueous Solutions Using $CoFe_{1.9}Mo_{0.1}O_4$ Magnetic Nanoparticles

I. A. Amar[1,2]*,A. Sharif[1], M. M. Alkhayali[1], M. A. Jabji[1], F. Altohami[1], M. A. Abdul Qadir[1] and M. M. Ahwidi[1]

[1] *Department of Chemistry, Faculty of Science, Sebha University, Sebha, Libya*
[2] *Central Laboratory at Sebha University, Sebha, Libya*

P A P E R I N F O

Paper history:
Received 02 October 2018
Accepted in revised form 31 December 2018

Keywords:
Spinel ferrite nanomaterial
Adsorption model
Dye removal
Adsorption kinetics
Adsorption isotherms

A B S T R A C T

In this study, the adsorption properties of spinel ferrite-based adsorbent, $CoFe_{1.9}Mo_{0.1}O_4$ (CFMo), for the removal of methylene blue (MB) from aqueous solution were investigated. Sol-gel process was successfully employed to prepare $CoFe_{1.9}Mo_{0.1}O_4$ magnetic nanoparticles. The synthesized adsorbent was characterized by Fourier transform infrared (FTIR), scanning electron microscope (SEM) and X-ray diffraction (XRD). The adsorption experiments were carried out at various operational conditions (solution pH, initial dye concentration, contact time, adsorbent dosage and temperature) to evaluate the potential adsorption property of CFMo magnetic nanoparticles. The results showed that, under the optimum adsorption parameters, approximately 95 % of MB dye can be removed. The adsorption data were described by Langmuir isotherm model and the maximum amount of MB adsorbed was about 20.45 mg/g. Several adsorption kinetic models and thermodynamic parameters (ΔG^o, ΔH^o, ΔS^o) were used to fit the adsorption experimental data. The adsorption kinetics followed the pseudo-second-order model (PSO), while the thermodynamic parameters indicate that the proposed adsorption process was endothermic and spontaneous in nature. The obtained results suggest that CFMo is promising adsorbent material for the removal of very toxic dyes from aqueous solutions.

***doi**: 10.5829/ijee.2018.09.04.04*

INTRODUCTION

Synthetic dyes are considered as one of the most dangerous water pollutants because of their detrimental effects on human health and aquatic life [1]. These organic dyes have been used extensively as colorants in many industries such as textile, leather, paper, plastics and cosmetics, etc. [2, 3]. These industries are responsible for discharging considerable amount of dye-contaminated water into aqueous systems [3, 4]. Most of these dyes are toxic in nature and have carcinogenic, mutagenic and teratogenic effects [5, 6]. Methylene blue (MB), known also as tetramethylthionine chloride (Figure 1), is a cationic dye which commonly used in textile industry for dyeing silk, wood and cotton. The acute exposure to MB can cause nausea, vomiting, increased heart rate, cyanosis, jaundice, profuse sweating, quadriplegia and mental confusion, etc. [2, 3]. Therefore, the treatment of effluents containing methylene blue before being released into aqueous systems is of environmental significance.

Various water treatment technologies have been developed in attempts to remove toxic synthetic dyes from contaminated water before drainage. These include; coagulation-flocculation, oxidation, membrane filtration, adsorption, ion-exchange, ozonation, photocatalytic degradation, electrochemical degradation and biological treatment [3, 4]. Compared to the aforementioned techniques, adsorption is preferred because of its unique properties such as; availability, simplicity of design, low operational cost, ease of operation, insensitivity to toxic pollutants, treating various types of dyes, no secondary pollutant formation and high removal efficiency [3, 5, 7-9]. Activated carbon (AC) is the most commonly used adsorbent by many dye manufacturing factories owing to its remarkable properties (e.g., porous structure, large surface area, good adsorption performance). However, the use of AC is limited due to the problems associated with its high production cost, sludge formation and regeneration or disposal [2, 5]. This highlights the need for exploring new adsorbents which are cheap, efficient and separated easily from adsorption media, easily recovered and reused.

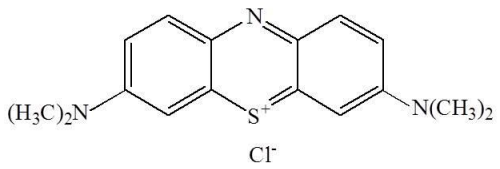

Figure 1. Molecular structure of methylene blue dye

*Corresponding author: I. A. Amar, E-mail: ibr.amar@sebhau.edu.ly

In recent years, magnetic nanoparticles (MNPs), in particular spinel ferrites nanoparticles (SFNPs), have attracted considerable attention due to their unique properties including; diverse structures, moderate saturation magnetization, chemical and thermal stabilities, small amount is required, high sensitivity, efficiency, cost-effective, fast adsorption kinetics, ease of functionalization, ease of recovery and reuse, no filtration is required and ease of separation after adsorption using an external magnetic field, etc[9-12]. In this regard, several spinel ferrites and spinel ferrite nanocomposites (SFNCs) including; $NiFe_2O_4$ [13], $MnFe_2O_4$ [14], $Mn_{0.2}Zn_{0.8}Fe_2O_4$ [15], $Mn_{0.6}Zn_{0.4}Fe_2O_4$/activated carbon [16] and XFe_2O_4/graphene oxide (X = Co, Mn, Ni) [17] have been employed as adsorbent materials for treating of methylene blue dye-contaminated water. Among spinel ferrites, cobalt ferrites ($CoFe_2O_4$) are regarded as promising candidate materials for the application as adsorbents in the field of water treatment technologies. In addition, it has been reported that the adsorption performance of $CoFe_2O_4$ could be enhanced by partial substitution of Fe^{3+} by other element (e.g., Pr^{3+}, Gd^{3+}, Al^{3+}, In^{3+}, Ni^{2+}, Cu^{2+}, etc.) [18-21]. In a recent study, Mohamed et al. [22] have successfully synthesized and studied the magnetic properties of Mo-substituted cobalt ferrite ($CoFe_{2-x}Mo_xO_4$, x = 0.04-0.3). Based on the previous discussion, it is expected that Mo-doped $CoFe_2O_4$would be a promising adsorbent material and can be employed for the removal of very toxic dyes from wastewater. However, to the best of our knowledge, there is no report on using Mo-doped $CoFe_2O_4$ magnetic nanoparticles as an adsorbent for the removal of methylene blue. Thus, the present work aims to synthesize Mo-substituted $CoFe_2O_4$ and to investigate its ability for removing of methylene blue from aqueous systems.

MATERIALS AND METODS

Materials

Methylene blue dye ($C_{16}H_{18}ClN_3S{\cdot}xH_2O$, x = 2-3) was purchased from ScP (Surechem products). Iron nitrate nonahydrate ($Fe(NO_3)_3{\cdot}9H_2O$) was purchased from Berck and Scientific Supplies. Cobalt nitrate ($Co(NO_3)_2{\cdot}6H_2O$) was purchased from Analyticals. Ammonium molybdate ($(NH_4)_6Mo_7O_{24}{\cdot}H_2O$), Hydrochloric acid (HCl) and sodium chloride (NaCl) were purchased from purchased from BDH Chemical. Citric acid ($C_6H_8O_7$) was purchased from Labkem. Sodium hydroxide (NaOH) was purchased from Fluka. Ethylene diamine tetraacetic acid, EDTA, ($C_{10}H_{18}N_2O_8$) was purchased from Serva. Amonia solution (35%) was purchased from Scharlau. All chemical in this work were used as supplied.

Synthesis of $CoFe_{1.9}Mo_{0.1}O_4$ nanoparticles

Spinel-based oxide nanoparticles in the form of $CoFe_{1.9}Mo_{0.1}O_4$ (CFMo) was synthesized via sol-gel process [23]. Initially, accurately weighed amounts of $Co(NO_3)_2{\cdot}6H_2O$, $Fe(NO_3)_3{\cdot}9H_2O$ and $(NH_4)_6Mo_7O_{24}{\cdot}H_2O$ were dissolved in a minimum amount deionized water. EDTA and citric acid were then added to the mixed solution as complexing agents at a molar ratio of metal cations: EDTA : citric acid of 1:1:1.5. The pH of the mixed solution was adjusted to around 6 by adding a diluted ammonia solution. The mixture was placed on a hot-plate and magnetically stirred under heating before getting a black sticky gel. Then, a solid product was obtained by further heating the gel precursor to dryness. Finally, the dried gel was heat treated in air at 600 ºC for 3 h to get the desired magnetic nanoparticles ($CoFe_{1.9}Mo_{0.1}O_4$).

Characterization of $CoFe_{1.9}Mo_{0.1}O_4$ nanoparticles

X-ray diffraction (XRD) pattern of $CoFe_{1.9}Mo_{0.1}O_4$ was collected at room temperature using a Philips – PW 1800 diffractometer with Ni-filtered CuKα radiation (λ=1.54186 Å) at scanning angle of 1.4 to 79.4º, with a step size of 0.02º. The lattice constant (*a*, Å) and the crystallite size (*D*, nm) of $CoFe_{1.9}Mo_{0.1}O_4$ nanoparticles were estimated using Equations 1 and 2, respectively [24].

$$a = d_{hkl}\sqrt{h^2 + k^2 + l^2} \quad (1)$$

$$D = \frac{0.9\lambda}{(\beta \cos\theta)} \quad (2)$$

where *khl* are the Miller indices, *d* is the interplanar distance, λ is the X-ray wavelength, θ is the Bragg angle for diffraction peak and β is the full width at half maximum (FWHM) for diffraction peak in radiance.

Fourier transform infrared spectrum (FTIR) of CFMo nanoparticles was recorded using KBr pellet method in the range of 400-4000 cm^{-1} using a Bruker Tensor 27 spectrophotometer. A LEO 1430PV Scanning Electron Microscope (SEM) was used to examine the surface morphology of the prepared adsorbent. The pH at the point zero charge (pHpzc) of the CFMo magnetic nanoparticles was determined using drift method [25]. The initial pH value (pH_i) of NaCl solution (0.1 mol/L) was adjusted to 3, 5, 7, 9, and 11 by adding either a 0.1 mol/L HCl or NaOH solution. Then, 0.1 g of CFMo magnetic nanoparticles was added to 25 mL of NaCl solution. After shaking for 24 h, the CFMo material easily separated magnetically from NaCl solution and the final pH value (pH_f) was determined. Finally, the pH_{PZC} was estimated from the intersection point of the plot of ΔpH (pH_i-pH_f) against pH_i [26].

Adsorption studies

a) Adsorption experiments

The stock solution of MB at concentration of 500 mg/L was prepared by dissolving accurately weighed amounts of MB into the required volume of deionized water. The desired concentrations of the working solutions were obtained by diluting the prepared stock solution. Batch mode was chosen to carry out all dye adsorption experiments and 25 mL Erlenmeyer flasks were used for this purpose. Each flask was filled with a 20 mL of MB solution, sealed tightly and placed in an orbital shaker (IKA-Werke) and shaken for a certain time at speed of 320 rpm. The adsorption experiments were carried out at varying operational conditions contact time (0-120 min), initial solution pH (3-11), adsorbent dosage (0.01-0.25 g 20/mL), initial MB concentration (50-250 mg/L) and solution temperature (25-45 ºC) to evaluate the suitability of CFMo nanoparticles as adsorbent for removing MB from aqueous solutions. The initial pH of dye solution was adjusted to the desired value by adding either 0.1 mol/L HCl or 0.1 mol/L NaOH using a pH-meter (Jenway model 3505, UK).

After each adsorption experiment, the residual concentration of MB in the solution was measured using a single beam UV-vis spectrophotometer (Jenway model 6305, UK) at the maximum wavelength (λ_{max}) of 662 nm [2]. The amount of MB adsorbed at any time t (q_t, mg/g), the amount of MB adsorbed at equilibrium (q_e, mg/g) and the percentage removal of MB (%R) were calculated using the following equations [6, 27]:

$$q_t = \frac{V(C_o - C_t)}{m} \quad (3)$$

$$q_e = \frac{V(C_o - C_e)}{m} \quad (4)$$

$$\%R = \frac{C_o - C_t}{C_o} \times 100 \quad (5)$$

where C_o is the initial dye concentrations (mg/L), C_t and C_e are the final dye concentration (mg/L) at any time t and at equilibrium, respectively. V is the volume of dye solution (L) and m is the adsorbent dose (g). The adsorption experiments were repeated three times and the data were reported as the mean ± SD.

b) Kinetic models

To better understand the adsorption process kinetics, two most widely used kinetic models including pseudo-first-order (PFO) [28] and pseudo-second-order (PSO) [29] were applied to fit the obtained experimental data.The linear forms of PFO (Equation 6) and PSO (Equation 7) can be expressed as follows [30]:

$$\ln\ (q_e - q_t) = \ln\ q_e - K_1 t \quad (6)$$

$$\frac{t}{q_t} = \frac{1}{K_2 q_e^2} + \frac{1}{q_e} t \quad (7)$$

where q_e and q_t are as indicated previously. K_1 (min^{-1}) and K_2 (g/mg min) are the rate constants PFO and PSO, respectively. From the intercept and slope of the plot of $\ln(q_e - q_t)$ versus t, respectively, the values of q_e and K_1 can be calculated. The intercept and the slop of plot of t/q_t versus t were used to calculate the values of K_2 and q_e, respectively.

c) Adsorption Isotherm models

In this study, Langmuir [31] and Freundlich [32], the most frequently isotherm models, were employed to describe the nature of the interaction between adsorbent and adsorbate. These empirical isotherm models were applied to fit the obtained experimental adsorption data at varying initial dye concentration (50-250 mg/L). Langmuir isotherm model is applicable for describing monolayer adsorption that occurs on homogenous surface [7]. Equation 8 expresses the linearized form of Langmuir equation, as described below [30]:

$$\frac{C_e}{q_e} = \frac{1}{q_{\max} K_L} + \frac{1}{q_{\max}} C_e \quad (8)$$

where $q_{\max}$ is the maximum amount of MB adsorbed (mg/g) and K_L is Langmuir constant (L/mg). From the linear plot of C_e against $C_e/q_{\max}$, the slope and the intercept can be used to calculated the values of $q_{\max}$ and K_L, respectively. The feasibility of Langmuir adsorption isotherm can be evaluated using a constant known as the separation factor (R_L). The value of R_L (dimensionless) can be calculated using following equation [30]:

$$R_L = \frac{1}{1 + K_L C_o} \quad (9)$$

The value of R_L indicates whether the type of the isotherm to be either favourable ($0 < R_L < 1$), unfavourable ($R_L > 1$), linear ($R_L = 1$) or irreversible ($R_L = 0$) [30].

Freundlich isotherm model is based on the assumption that the multilayer of the adsorption process takes place on heterogeneous surface [7]. The linearized form of Freundlich equation is as given below [30]:

$$\ln q_e = \ln K_F + \frac{1}{n} \ln C_e \quad (10)$$

where K_F is Freundlich constant ((mg/g)/(mg/L)^n), n is the adsorption intensity (dimensionless) that indicates the surface heterogeneity. The values of n can be also used to verify types of adsorption. The adsorption process is linear ($n = 1$), unfavourable ($n > 1$), favourable ($n < 1$) and irreversible ($n = 1$) [30]. The value of n was calculated from the slope ($1/n$), while the value of K_F were calculated from the intercept ($\ln K_F$) of the linear plot of $\ln C_e$ against $\ln q_e$.

d) Adsorption thermodynamics

The thermodynamic parameters such as Gibb's free energy (ΔG^o), enthalpy (ΔH^o) and entropy (ΔS^o) were determined using the following equations [30, 33]:

$$\Delta G^o = \Delta H^o - T\Delta S^o \quad (11)$$

$$\ln K_C = \frac{-\Delta H^o}{R}\frac{1}{T} + \frac{\Delta S^o}{R} \quad (12)$$

$$K_C = \frac{C_S}{C_e} \quad (13)$$

where K_C is a constant called the distribution coefficient and determined using Equation 13, C_S is the MB concentration (mg/L) on the adsorbent surface, T is absolute temperature (K). and R is the gas constant (8.314 J/mol/K). The slope and the intercept of the plot of $\ln K_C$ versus ($1/T$) were used to calculate the values of ΔH^o (kJ/mol) and ΔS^o (kJ/mol), respectively.

RESULTS AND DISCUSSION

Characterization of the adsorbent

Figure 2 represents the characteristics of the prepared adsorbent ($CoFe_{1.9}Mo_{0.1}O_4$, CFMo). Figure 2a shows the XRD pattern of $CoFe_{1.9}Mo_{0.1}O_4$ magnetic nanoparticles after firing its corresponding ash in air at 600 ºC for 3 h. As shown from the XRD pattern, all diffraction peaks are well indexed to characteristic reflections of magnetite with a cubic structure (JCPDS card No. 19-0629). In addition, no extra peaks were observed indicating the formation of a single phase of spinel ferrites (CFMo). The XRD data of the strongest peak (311) were used to calculate the values of CFMo structural parameters including lattice constant (a), the

volume of the unit cell (a^3) and crystallite size (D). The calculated values of a, a^3 and D were found to be 8.2786 Å, 567.38 (Å)^3 and 47.40 nm, respectively.

Figure 2b shows the FTIR spectrum of CFMo nanoparticles. As can be seen from the spectrum, the characteristic band of all spinel ferrites was observed at 586 cm^{-1}. This absorption band is ascribed to metal-oxygen (Fe-O) vibration. The observed peaks in the range of 815 to 1122 cm^{-1} can be assigned to NO_3^- group vibration. In addition, the band located at 1632 cm^{-1} is ascribed to O-H bending vibrations, while that observed at 3415 cm^{-1} is assigned to O-H stretching vibrations [27, 34, 35]. Figure 2c shows the SEM image of $CoFe_{1.9}Mo_{0.1}O_4$ magnetic nanoparticles. As shown, the morphology of the prepared adsorbent (CFMo) consists of a heterogonous nanostructure. It can be also seen from the SEM image that CFMo magnetic nanoparticles form some agglomerates as a result of their particle-particle interactions [19, 35]. The pH at the point zero charge (pH_{PZC}) of CFMo nanoparticles was found to 6.35 as presented in Figure 2d.

Effect of operational parameters on dye adsorption

a) Effect of solution pH

The effect of the solution pH was investigated by varying the pH values from 3 to 11 at a fixed initial MB concentration of 100 mg/L, adsorbent dose of 0.01 g 20/mL and over a period of 60 min. As mentioned previously, HCl and NaOH were used to adjust the solution pH to the desired value.

The removal efficiency or percentage removal of MB (%R) and the amount adsorbed of MB (q_t, mg/g) as a function of dye solution pH are shown in Figure 3. It can be clearly seen that, the %R and q_t increased significantly with increasing solution pH and reaching maximum values at pH 7. However, by further increasing the dye solution pH from 7 to 11, a decrease in the values of %R and q_t were observed. MB is a cationic dye and gives positively charged ions when dissolve in water [36]. In addition, the pH_{PZC} value of CFMo

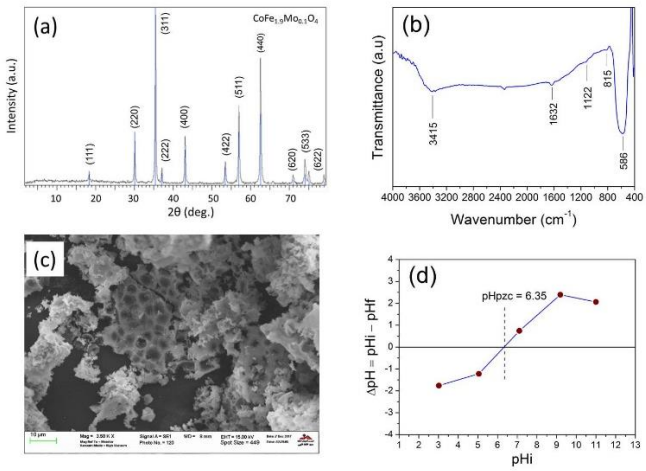

Figure 2. (a) Powder X-ray diffraction pattern; (b) FTIR spectrum; (c) SEM image; (d); the point of zero charge of $CoFe_{1.9}Mo_{0.1}O_4$magnetic nanoparticles

nanoparticles was about 6.35 (Figure 2d). This means that the adsorbent (CFMo) surface will be positively charged at pH < pH_{PZC} and negatively charged at pH > pH_{PZC} [10]. Thus, the low q_t and %R values that observed at pH < 6.35 can be explained considering electrostatic repulsion between the adsorbent surface (positively charged) and MB cations (positive ions). On the other hand, the high %R and q_t values at pH 7 (pH > 6.35) could be due to the increase in the electrostatic attraction between the cationic dye (positive ions) and the negatively charged surface of CFMo. As reported by Al-Anber et al. [37], MB dye which contains Cl^-(MB-S^+Cl^-) and NaOH (for pH adjustment) are expected to undergo replacement reaction and resulting in the formation of NaCl and (MB-S^+OH^-). Therefore, the decreased values of %R and q_t at pH values above 7 (pH > pH_{PZC}) could be due to the increase in the solution ionic strength as a result of NaCl formation.

b) Effect of contact time

The effect of contact time on the q_t (mg/g) and %R of MB was investigated by changing the contact time and keeping the other experimental parameters at constant values (pH value 7, adsorbent dose of 0.01 g/20 mL and initial MB concentration of 100 mg/L) and the results are shown in Figure 4.

As can be seen, the q_t value is increased with increasing the contact time and reaching a maximum value of about 98.40 mg/g at 30 min. However, when the contact time was further increased above 30 min, the q_t value decreased slightly (almost to a constant value), which may due to saturation of all available active binding sites [38]. It can also be seen from Figure 4 that the maximum %R value (43%) was attained at 60 min period of time.

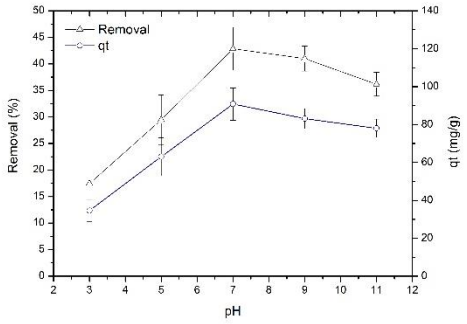

Figure 3. Effect of initial pH on the MB removal percentage and adsorption capacity

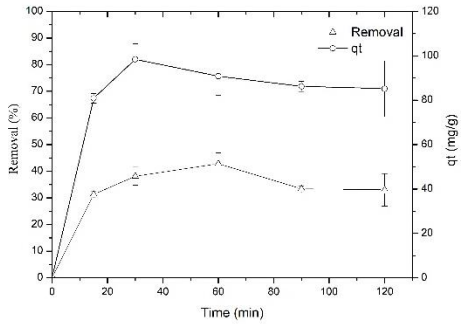

Figure 4. Effect of the contact time on the MB removal percentage and adsorption capacity

c) Effect of adsorbent dose

The effect of CFMo quantity on the %R of MB dye and the equilibrium adsorption capacity (q_e, mg/g) was investigated in batch experiment by varying the amount of the adsorbent

(CFMo) from 0.01 to 0.25 g/20 mL and keeping the other parameters constant (dye solution pH at 7, dye concentration at 100 mg/L and contact time at 60 min). As can be seen from Figure 5, the %R of MB increased significantly from 38.94 % (adsorbent dose 0.01 g/20 mL) to 95.35 % (adsorbent dose 0.20 g/20 mL). This could be due to the fact that the numbers of binding sites which are available for adsorbing MB molecules are increased as the adsorbent dose is increased [6]. However, by further increasing the adsorbent dose above 0.15 g/20 mL, no significant increase in the %R of MB was observed and a highest value of about 95.35 % was obtained at adsorbent amount of 0.20 g/20 mL. Therefore, this optimum adsorbent dose (0.20 g/20 mL) was used for the subsequent experiments. It can be also seen from Figure 5, that increasing the amount of the adsorbent from 0.01 to 0.25 g/20 mL leads to a significant decrease in the q_e from 96.63 to 8.28 mg/g. This could be due to the fact that, during adsorption process, the available adsorption sites remain unsaturated [39].

d) Effect of the initial dye concentration

The effect of the initial dye concentration was studied by varying MB concentration from 50 to 250 mg/L and keeping the other operational condition at the optimized values. Figure 6 shows the dependence of the %R and the q_e of MB dye on the initial MB concentration. As can be seen, no significant difference in the %R of MB was observed with increasing the initial concentration from 50 to 100 mg/L. However, the %R of MB decreased as the initial concentration was further increased from 100 to 250 mg/L and reached a minimum value of about 70.84 % at 250 mg/L. This decrease could be due to the fact that the active adsorption sites of the adsorbent (CFMo) became saturated after adsorption of certain concentration of MB [40].

Therefore, the optimum MB concentration was chosen to be 100 mg/L. In contrast to the %R of MB, the q_e value increased significantly from 4.89 to 19.12 mg/g as the initial dye concentration was increased from 50 to 250 mg/L, as shown in Figure 6. This can be explained by the fact that, at a fixed adsorbent dose, the high initial concentration of the dye will provide the required driving to transfer the MB molecules from the bulk liquid phase to the surface of solid adsorbent [8, 41, 42]. In addition, the increase in the value of

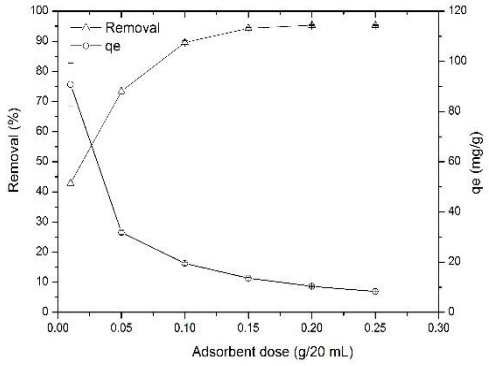

Figure 5. Effect of the adsorbent dose on the MB removal percentage and adsorption capacity

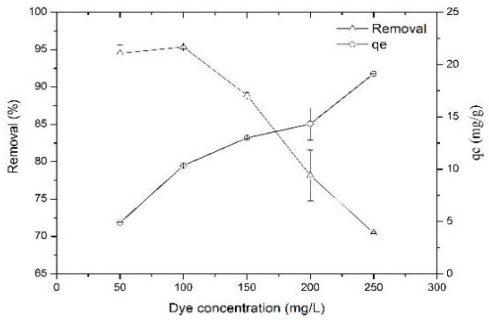

Figure 6. Effect of the initial dye concentration on the MB removal percentage and adsorption capacity

q_e might be due to the enhancement in the adsorbent-dye interaction as a consequence of increasing the initial dye concentration [8].

e) Effect of solution temperature

The effect of solution temperature on adsorption process of MB dye onto CFMo magnetic nanoparticles was investigated at various temperatures (25, 35 and 45 °C) and under the above mentioned optimized operational conditions. As can be seen from Figure 7, increasing the solution temperature resulted in decreasing both the %R of MB and the q_e value. This might be due to fact that, by increasing the solution temperature, the kinetic energy of dye molecules will be increased, thus weakening the interaction between the dye molecules and the binding sites of the adsorbent magnetic nanoparticles [39]. This decrease in the %R and q_e values with temperature indicates the exothermic nature of the proposed adsorption process [7].

Adsorption kinetics

The adsorption kinetic of MB on the surface of CFMo was evaluated by linear pseudo-first-order (PFO) and pseudo-second-order (PSO) models (Figure S1). The fitting parameters of the models are listed in Table 1.

In contrast to the PFO model, the calculated q_e value obtained from PSO model is close to the experimental q_e value (Table 1). It can also be seen from Table 1 that, the correlation coefficient (R^2) value of PSO model (0.9975) is higher than that of PFO. This means that the proposed adsorption process is better described by the PSO kinetic model.

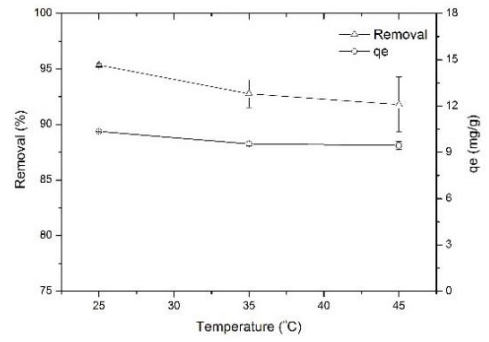

Figure 7. Effect of solution temperature on the MB removal percentage and adsorption capacity

Adsorption isotherms

Langmuir and Freundlich isotherm models were used to fit the experimental adsorption data of MB onto CFMo nanoparticles (Figure S2). Table 2 lists the calculated parameters of these isotherm models. The calculated values of separation factor (R_L) at different initial dye concentration (50-250 mg/L) were less than unity (0.151-0.033). This indicates the favourability of Langmuir isotherm to describe the adsorption process [7]. It is to be also noted from Table 2 that, the correlation coefficient (R^2) value of Langmuir isotherm model (0.9706) is higher than that of Freundlich isotherm model (0.7788). This suggests that the Langmuir isotherm model is favourable to describe the adsorption process. In addition, the maximum adsorbed amount of MB (q_{max}) determined from Langmuir isotherm was about 20.45 mg/g. Table 3 represents a comparison of the maximum adsorbent amount of MB onto different adsorbents [2, 13-15, 43-45]. The obtained results suggest that CFMo is promising adsorbent material for the removal of very toxic cationic dye (MB) from wastewater.

Adsorption Thermodynamics

The Gibb's free energy (ΔG^o) was calculated using Equation 11, whereas the values of the (ΔS^o) and enthalpy (ΔH^o) respectively, were calculated from the intercept and slope of Van't Hoff plot of $\ln K_C$ versus $1/T$ (Figure S3). Table 4 lists the values of the calculated thermodynamic parameters. The value of ΔG^o was negative, indicating the feasibility and the spontaneous nature of the proposed adsorption process. The observed decrease in negative values of ΔG^o with the increase in the dye solution temperature implies that higher temperature is less favourable for the MB adsorption. The negative value of ΔH^o substantiated the exothermic nature of MB adsorption process. Furthermore, the obtained value of ΔH^o was found to be -24.17 kJ/mol, indicating a physical adsorption

TABLE 1. Kinetic parameters for the adsorption of MB onto CFMo nanoparticles

q_e, exp (mg/g)	Pseudo-first-order		
	q_e, cal (mg/g)	k_1 (min^{-1})	R^2
90.94	39.26	1.28×10^{-2}	0.2513
	Pseudo-second-order		
	q_e, cal (mg/g)	k_2 (g/mg.min)	R^2
	85.25	9.04×10^{-3}	0.9975

TABLE 2. Adsorption isotherm parameters for adsorption of MB onto CFMo nanoparticles

Langmuir isotherm		
q_{max} (mg/g)	K_L (L/mg)	R^2
20.45	0.109	0.9706
Freundlish isotherm		
K_F (mg/g)/(mg/L)^n	n	R^2
4.50	2.95	0.7788

TABLE 3. Comparison of the maximum adsorption capacities of MB onto various adsorbents

Adsorbent	q_{max} (mg/g)	Reference
PANI-$NiFe_2O_4$	3.31	[43]
ZMC	4.44	[2]
CLP	6.36	[2]
$CoFe_2O_4$/MWCNTs	14.28	[44]
$CoFe_{1.9}Mo_{0.1}O_4$	20.45	This study
$MnFe_2O_4$	20.7	[14]
ZnO/$ZnFe_2O_4$	37.27	[45]
$Mn_{0.2}Zn_{0.8}Fe_2O_4$	40.97	[15]
$NiFe_2O_4$	138.5	[13]

PANI = Polyaniline-Nickel, ZMC = Zea Mays Cobs, CLP = Citrus Limetta Peel, MWCNTs = Malti-Walled Carbon Nanotubes.

TABLE 4. Thermodynamic parameters for adsorption of MB onto CFMo nanoparticles

ΔH^o (kJ/mol)	ΔS^o (J/mol.K)	ΔG^o (kJ/mol)		
		298 K	308 K	318 K
-24.04	-55.98	-7.36	-6.80	-6.24

mechanism. The negative ΔS^o value suggests the decrease in randomness at the solid-liquid interface during the adsorption of MB on CFMo. The thermodynamic findings are similar to that obtained for the adsorption of MB by citric acid modified peanut shell [46].

CONCLUSION

In summary, spinel ferrite magnetic nanoparticles ($CoFe_{1.9}Mo_{0.1}O_4$, CFMo) were successfully synthesized via a sol-gel process. The XRD revealed that a single-phase spinel oxide was obtained when the gel precursor was calcined in air at 600 ºC for 3 h. The adsorption property of CFMo for the removal of MB was investigated under different operational conditions, while about 95 % of MB was removed at pH of 7, contact time of 60 min, adsorbent dosage of 0.2 g/20 mL, initial dye concentration of 100 mg/L and room temperature (25 ºC). The kinetic studies revealed that the data followed the pseudo-second-order kinetic model. The equilibrium of adsorption of MB onto CFMo was better described by Langmuir isotherm model and the maximum adsorbed amount of MB was found to be 20.45 mg/g.The thermodynamic studies indicated that the adsorption of MB onto CFMo was feasible, spontaneous, physical and exothermic in nature. The obtained results suggest that CFMo is promising adsorbent for the adsorptive removal of toxic dyes from wastewater.

ACKNOWLEDGEMENTS

The authors would like to thank the Department of Chemistry, Sebha University, Libya for the financial support of this work. The authors are thankful to Libyan Petroleum Institute,

Tripoli, Libya for performing XRD and SEM analysis. The authors also thank Mr. FathiElsharif and Mr. Khaled Azzabi from the Nuclear Research Center, Tajoura, Libya for performing FTIR analysis.

CONFLICT OF INTEREST

We have no conflicts of interest to disclose.

REFERENCES

1. Santhosh, C., V. Velmurugan, G. Jacob, S.K. Jeong, A.N. Grace and A. Bhatnagar, 2016. Role of nanomaterials in water treatment applications: A review. Chemical Engineering Journal, 306: pp. 1116-1137.
2. Singh, H., G. Chauhan, A.K. Jain and S.K. Sharma, 2017. Adsorptive potential of agricultural wastes for removal of dyes from aqueous solutions. Journal of Environmental Chemical Engineering, 5(1): pp. 122-135.
3. Rafatullah, M., O. Sulaiman, R. Hashim and A. Ahmad, 2010. Adsorption of methylene blue on low-cost adsorbents: A review. Journal of Hazardous Materials, 177(1–3): pp. 70-80.
4. Ahmed, A., S.H. Mohd-Setapar, C.S. Chuon, A. Khatoon, W.A. Wani, R. Kumar and M. Rafatullah, 2015. Recent advances in new generation dye removal technologies: noval search for approaches to repocess wastewater. RSC Advances, 5: pp. 30801-30818.
5. Tan, K.B., M. Vakili, B.A. Horri, P.E. Poh, A.Z. Abdullah and B. Salamatinia, 2015. Adsorption of dyes by nanomaterials: Recent developments and application mechanisms. Separation and Purification Technology 150: pp. 229-242.
6. Moeinpour, F., A. Alimoradi and M. Kazemi, 2014. Efficient removal of Eriochrome black-T from aqueous solution using $NiFe_2O_4$ magnetic nanoparticles. Journal of Environmental Health Science and Engineering, 12(1): pp. 112.
7. Mahto, T.K., A.R. Chowdhuri and S.K. Sahu, 2014. Polyaniline-functionalized magnetic nanoparticles for the removal of toxic dye from wastewater. Journal of Applied Polymer Science, 131(19).
8. Dawood, S., T.K. Sen and C. Phan, 2014. Synthesis and characterisation of novel-activated carbon from waste biomass pine cone and its application in the removal of congo red dye from aqueous solution by adsorption. Water, Air, & Soil Pollution, 225(1): pp. 1818.
9. Kefeni, K.K., B.B. Mamba and T.A.M. Msagati, 2017. Application of spinel ferrite nanoparticles in water and wastewater treatment: A review. Separation and Purification Technology, 188: 399-422.
10. Reddy, D.H.K. and Y.-S. Yun, 2016. Spinel ferrite magnetic adsorbents: alternative future materials for water purification? Coordination Chemistry Reviews, 315: pp. 90-111.
11. Mehta, D., S. Mazumdar and S.K. Singh, 2015. Magnetic adsorbents for the treatment of water/wastewater—A review. Journal of Water Process Engineering, 7: pp. 244-265.
12. Gomez-Pastora, J., E. Bringas and I. Ortiz, 2014. Recent progress and future challenges of high performance magnetic nano-adsorbent in environmental applications. Chemical Engineering Journal, 256: 187-204.
13. Hou, X., J. Feng, X. Liu, Y. Ren, Z. Fan, T. Wei, J. Meng and M. Zhang, 2011. Synthesis of 3D porous ferromagnetic $NiFe_2O_4$ and using as novel adsorbent to treat wastewater. Journal of colloid and interface science, 362(2): pp. 477-485.
14. Hou, X., J. Feng, Y. Ren, Z. Fan and M. Zhang, 2010. Synthesis and adsorption properties of spongelike porous $MnFe_2O_4$. Colloids and Surfaces A: Physicochemical and Engineering Aspects, 363(1): 1-7.
15. Hou, X., J. Feng, X. Liu, Y. Ren, Z. Fan and M. Zhang, 2011. Magnetic and high rate adsorption properties of porous $Mn_{1-x}Zn_xFe_2O_4$ ($0 \leqslant x \leqslant 0.8$) adsorbents. Journal of colloid and interface science, 353(2): pp. 524-529.
16. Wang, R., J. Yu and Q. Hao, 2018. Activated carbon/$Mn_{0.6}Zn_{0.4}Fe_2O_4$ composites: Facile synthesis, magnetic performance and their potential application for the removal of methylene blue from water. Chemical Engineering Research and Design, 132: pp. 215-225.
17. Bach, L.G., T.V. Tran, T.D. Nguyen, T.V. Pham and S.T. Do, 2018. Enhanced adsorption of methylene blue onto graphene oxide-doped XFe_2O_4 (X = Co, Mn, Ni) nanocomposites: kinetic, isothermal, thermodynamic and recyclability studies. Research on Chemical Intermediates, 44: pp. 1661-1687.
18. Zhang, L., J. Lian, L. Wang, J. Jiang, Z. Duan and L. Zhao, 2014. Markedly enhanced coercive field and Congo red adsorption capability of cobalt ferrite induced by the doping of non-magnetic metal ions. Chemical Engineering Journal (2014), pp. 241: 384–392.
19. Farooq, S., A. Saeed, M. Sharif, J. Hussain, F. Mabood and M. Iftekhar, 2017. Process optimization studies of crystal violet dye adsorption onto noval, mixed metal $Ni_{0.5}Co_{0.5}Fe_2O_4$ ferrospinel nanoparticles using factorial design. Journal of Water Process Engineering, 16: 132-141.
20. Zhao, X., W. Wang, Y. Zhang, S. Wu, F. Li and J.P. Liu, 2014. Synthesis and characterization of gadolinium doped cobalt ferrite nanoparticles with enhanced adsorption capability for Congo Red. Chemical Engineering Journal, 250: 164–174.
21. Wu, X., Z. Ding, N. Song, L. Li and W. Wang, 2016. Effect of the rare-earth substitution on the structural, magnetic and adsorption properties in cobalt ferrite nanoparticles. Ceramics International, 42: 4246-4255.
22. Mohamed, M.B., A.M. Wahba and M. Yehia, 2014. Structural and magnetic properties of $CoFe_{2-x}Mo_xO_4$ nanocrystalline ferrites. Materials Science and Engineering B, 190: 52-58.
23. Ling, Y., J. Yu, B. lin, X. Zhang, L. Zhao and X. Liu, 2011. A cobalt-free $Sm_{0.5}Sr_{0.5}Fe_{0.8}Cu_{0.2}O_{3-\delta}$-$Ce_{0.8}Sm_{0.2}O_{2-\delta}$ composite cathode for proton-conducting solid oxide fuel cells. Journal of Power Sources 196: 2631-2634.
24. Fu, Y.-P., S.-H. Chen and J.-J. Huang, 2010. Preparation and characterization of $Ce_{0.8}M_{0.2}O_{2-\delta}$ (M = Y, Gd,Sm, Nd, La) solid electrolyte materials for solid oxide fuel cells. International Journal of Hydrogen Energy, 35: 745-752.
25. Kosmulski, M., (2009). pH-dependent surface charging and points of zero charge. IV. Update and new approach. Journal of Colloid and Interface Science, 337(2): 439-448.
26. Tran, H.N., Y.-F. Wang, S.-J. You and H.-P. Chao, 2017. Insights into the mechanism of cationic dye adsorption on activated charcoal: The importance of π–π interactions. Process Safety and Environmental Protection, 107: 168-180.
27. Konicki, W., D. Sibera, E. Mijowska, Z. Lendzion-Bieluń and U. Narkiewicz, 2013. Equilibrium and kinetic studies on acid dye Acid Red 88 adsorption by magnetic $ZnFe_2O_4$ spinel ferrite nanoparticles. Journal of colloid and interface science, 398: 152-160.
28. Lagergren, S., 1898. About the Theory of so-called Adsorption of Soluble Substances. Kungliga Sevenska Vetenskapasakademiens Handlingar, 24: 1-39.
29. Ho, Y.S. and G. McKay, 1999. Pseudo-second order model for sorption processes. Process Biochemistry, 34: 451-465.
30. Tran, H.N., S.-J. You, A. Hosseini-Bandegharaei and H.-P. Chao, 2017. Mistakes and inconsistencies regarding adsorption of contaminants from aqueous solutions: A critical review. Water Research, 120: 88-116.
31. Langmuir, I., 1916. The constitution and fundamental properties of solids and liquids. Part I. Solids. . The Journal of the American Chemical Society, 38: pp. 2221-2295.
32. Freundlich, H.M.F., 1906. Over the adsorption in solution. The Journal of Physical Chemistry, 57: 385-470.
33. Bonetto, L.R., F. Ferrarini, C.D. Marco, J.S. Crespo, R. Guégan and M. Giovanela, 2015. Removal of methyl violet 2B dye from aqueous solution using a magnetic composite as an adsorbent. Journal of Water Process Engineering, 6: pp. 11-20.
34. Stoia, M. and C. Muntean, 2015. Preparation, Characterization and Adsorption Properties of MFe_2O_4 (M = Ni, Co, Cu) Nanopowers. Environmental Engineering and Managment Journal, 14(6): 1247-1259.
35. Wang, W., Z. Ding, M. Cai, H. Jian, Z. Zeng, F. Li and J.P. Liu, 2015. Synthesis and high-efficiency methylene blue adsorption of magnetic PAA/$MnFe_2O_4$ nanocomposites. Applied Surface Science, 346: pp. 348-353.

36. Zayed, M.F., W.H. Eisa and B. Anis, 2016. Removal of methylene blue using Phoenix dactylifera/PVA composite; an eco-friendly adsorbent. Desalination and Water Treatment, 57(40): 18861-18867.
37. Al-Anber, Z.A., M.A. Al-Anber, M. Matouq, O. Al-Ayed and N.M. Omari, 2011. Defatted Jojoba for the removal of methylene blue from aqueous solution: Thermodynamic and kinetic studies. Desalination, 276(1–3): 169-174.
38. Erol, K., K. Köse, D.A. Köse, Ü. Sızır, İ. Tosun Satır and L. Uzun, 2016. Adsorption of Victoria Blue R (VBR) dye on magnetic microparticles containing Fe (II)–Co (II) double salt. Desalination and Water Treatment, 57(20): 9307-9317.
39. Mahida, V.P. and M.P. Patel, 2016. Removal of some most hazardous cationic dyes using novel poly (NIPAAm/AA/N-allylisatin) nanohydrogel. Arabian Journal of Chemistry, 9(3): 430-442.
40. Chawla, S., H. Uppal, M. Yadav, N. Bahadur and N. Singh, 2017. Zinc peroxide nanomaterial as an adsorbent for removal of Congo red dye from waste water. Ecotoxicology and Environmental Safety, 135: 68-74.
41. Abbas, M. and M. Trari, 2015. Kinetic, equilibrium and thermodynamic study on the removal of Congo Red from aqueous solutions by adsorption onto apricot stone. Process Safety and Environmental Protection, 98: 424-436.
42. Deb, A., M. Kanmania, A. Debnath, K.L. Bhowmik and B. Saha, 2017. Preparation and characterization of magnetic $CaFe_2O_4$ nanoparticles for efficient adsorption of toxic Congo Red dye from aqueous solution: predictive modeling by artificial neural network. Desalination and Water Treatment, 89: 197–209.
43. Patil, M.R. and V. Shrivastava, 2016. Adsorptive removal of methylene blue from aqueous solution by polyaniline-nickel ferrite nanocomposite: a kinetic approach. Desalination and Water Treatment, 57(13): 5879-5887.
44. Farghali, A., M. Bahgat, W. El Rouby and M. Khedr, 2012. Decoration of MWCNTs with $CoFe_2O_4$ nanoparticles for methylene blue dye adsorption. Journal of solution chemistry, 41(12): 2209-2225.
45. Feng, J., Y. Wang, L. Zou, B. Li, X. He, Y. Ren, Y. Lv and Z. Fan, 2015. Synthesis of magnetic $ZnO/ZnFe_2O_4$ by a microwave combustion method, and its high rate of adsorption of methylene blue. Journal of colloid and interface science, 438: 318-322.
46. Wang, P., Q. Ma, D. Hu and L. Wang, 2016. Adsorption of methylene blue by a low-cost biosorbent: citric acid modified peanut shell. Desalination and Water Treatment, 57(22): 10261-10269.

Persian Abstract

DOI: 10.5829/ijee.2018.09.04.04

چکیده

در این پژوهش، خواص جذب جاذب بر پایه فریت اسپینل (CFMo) $CoFe1.9Mo0.1O4$، به منظور حذف متیلن بلو (MB) از محلول آبی مورد ارزیابی قرار گرفت. فرایند سل-ژل به طور موفقی برای تهیه نانوذرات آهنربایی $CoFe1.9Mo0.1O_4$ به کار گرفته شد. خصوصیات جاذب سنتز شده از طریق طیف سنجی مادون قرمز (FTIR)، میکروسکوپ الکترونی روبشی (SEM) و پراش اشعه ایکس (XRD) شناسایی گردید. آزمایشات جذب در شرایط عملیاتی مختلف (pH محلول، غلظت رنگ اولیه، زمان تماس، میزان جاذب و دما)، جهت ارزیابی ظرفیت جذب نانوذرات آهنربایی CFMo انجام شد. نتایج حاکی از آن است که تحت پارامترهای بهینه جذب، حدود ۹۵٪ از رنگ MB می‌تواند حذف شود. داده‌های جذب با استفاده از مدل ایزوترم لانگ‌مویر توصیف گردید و حداکثر میزان MB جذب شده حدود ۲۰/۴۵ mg/g گزارش شد. چندین مدل سینتیکی جذب و پارامترهای ترمودینامیکی (ΔG^o، ΔH^o و ΔS^o) برای تطبیق داده‌های تجربی جذب استفاده گردید. سینتیک جذب از یک مدل درجه شبه دو (PSO) تبعیت نموده، و پارامترهای ترمودینامیکی نشان می‌دهد که فرایند جذب پیشنهادی، به صورت گرماگیر و خودبخودی رخ می‌دهد. نتایج حاصل بیانگر آن است که CFMo ترکیب جاذب امیدبخشی برای حذف رنگ‌های بسیار سمی از محیط‌های آبی می‌باشد.